J Musculoskelet Neuronal Interact 2008; 8(1):71-78

Original Article

Hylonome

Site specific bone adaptation response to mechanical loading

S.J. Kuruvilla, S.D. Fox, D.M. Cullen, M.P. Akhter

Creighton University, Omaha, NE, USA

Abstract

Over 25 million Americans suffer from osteoporosis. Bone size and strength depends both upon the level of adaptation due to physical activity (applied load), and genetics. We hypothesized that bone adaptation to loads differs among mice breeds and bone sites. Forty-five adult female mice from three inbred strains (C57BL/6 [B6], C3H/HeJ [C3], and DBA/2J [D2]) were loaded at the right tibia and ulna *in vivo* with non-invasive loading devices. Each loading session consisted of 99 cycles at a force range that induced ~2000 microstrain (με) at the mid-shaft of the tibia (2.5 to 3.5 N force) and ulna (1.5 to 2 N force). The right and left ulnae and tibiae were collected and processed using protocols for histological undecalcified cortical bone slides. Standard histomorphometry techniques were used to quantify new bone formation. The histomorphometric variables include percentage mineralizing surface (%MS), mineral apposition rate (MAR), and bone formation rate (BFR). Net loading response [right-left limb] was compared between different breeds at tibial and ulnar sites using two-way ANOVA with repeated measures ($p<0.05$). Significant site differences in bone adaptation response were present within each breed ($p<0.005$). In all the three breeds, the tibiae showed greater percentage MS, MAR and BFR than the ulna at similar *in vivo* load or mechanical stimulus (strain). These data suggest that the bone formation due to loading is greater in the tibiae than the ulnae. Although, no significant breed-related differences were found in response to loading, the data show greater trends in tibial bone response in B6 mice as compared to D2 and C3 mice. Our data indicate that there are site-specific skeletal differences in bone adaptation response to similar mechanical stimulus.

Keywords: Mechanical Loading, Bone Adaptation, B6, D2, C3, Mice

Introduction

Osteoporosis is a critical bone disease affecting >25 million Americans which leads to skeletal fragility[1,2]. People with osteoporosis suffer from significantly decreased bone mass and density, thus increasing their risk for fragility fractures. The severity of osteoporosis varies with genetics and lifestyle[2-6]. For instance, the increased fragility fracture risk in Caucasian women is greater than African American women[7] and greater in smokers than non-smokers[3-6].

The risk of fragility fractures can be reduced by some treatments including chemicals (drugs) and mechanical interventions (exercise). PTH compounds have been shown to increase bone mass in humans[8-11] and in animal models[12,13]. The mechanical loading of the skeleton via exercise has also improved bone mass in human[14-16] and animal models[17-28]. These data suggest that bone mass and structure are functions of mechanical stimuli or deformation as experienced during daily living. Therefore, it has been widely accepted that exercise-related bone adaptation results in increased bone mass and structure, improves overall bone strength and reduces bone fragility fracture risk[17,29,30].

Increased bone mass and size due to mechanical stimuli has been shown in several animal models, suggesting that bone adaptation response is dependent upon the magnitude of mechanical stimuli (mechanical deformation or strain)[31,32]. These models also suggest that a minimum threshold mechanical stimuli is required to illicit an osteogenic bone adaptation response[33,34]. The bone adaptation response is in the form of lamellar or woven bone. The lamellar bone response results in layers of organized bone due to mechanical strain of less than 2000 microstrain[33-36]. While the woven bone is disorganized, it is a rapid response due to induced mechanical strain greater than 3500 microstrain[34,36].

The authors have no conflict of interest.

Corresponding author: MP Akhter, Ph.D., ORC, Creighton University, Suite 4820, 610 N, 30th Street, Omaha, NE 68131, USA
E-mail: akhtermp@creighton.edu

Accepted 15 August 2007

Due to the increases in mechanical strain, osteoblast activity increases which causes bone formation[34,35] that results in stronger and larger bones. These effects have been demonstrated in both mouse and rat studies, where animals were subjected to non-invasive external mechanical forces using a four-point bending device[23-26,37-39]. Li et al. 2003[40] reported histomorphometry data from tibial and ulnar loading within each rat without the site-specific comparison of the periosteal surfaces. Although site-specific bone adaptation response was noted in a human study[29,41], and in a mouse tibia model (cortical vs. cancellous)[42,43], we do not know if various skeletal sites (tibia vs. ulnae) in the same animal will respond differently to similar mechanical stimulus or strain. In addition, Sheng et al.[44] reported site-specific differences in bone formation rate with higher rates at vertebral bodies than in femoral trabecular bone suggesting possible differences in the bone formation response to mechanical stimulus at various skeletal sites. The objective of this study was to measure site- and breed/genetic-specific bone response to a given mechanical stimulus in mice. Bone adaptation response to known mechanical stimuli was investigated at tibial and ulnar sites of mice from 3 different genotypes (breeds). Future studies should be done to see what other important factors can be found and even manipulated, which will enhance the bone adaptation response to exercise (mechanical stimulus).

This paper investigates whether the bone adaptation response is site-specific and whether it is dependent on the breed. We used two bone sites, the right tibia and right ulna, in three mouse breeds that included: 1) C57BL/6J [B6], 2) DBA/2J [D2] and 3) C3H/HeJ [C3].

Materials and methods

A. Animals

This experiment used 16-week-old virgin female mice from 3 breeds. There were 15 mice from each breed C57BL/6[B6], DBA/2[D2] and C3H/He[C3]. The animals were purchased from Jackson Lab (Bar Harbor, Main) and housed at Creighton University animal facility for the duration of this experiment. The animals were fed a standard rodent diet and water *ad libitum*. Creighton University's Animal Care and Use Committee approved the animal protocols.

B. *In vivo* loading

In vivo loadings of both tibia and ulna were performed one at a time by a load controlled electromagnetic loading device similar to one used in other studies[21,28]. The *in vivo* loadings were done at 99 cycles per day; 3 days a week for twenty-one days using a 2Hz (2 cycles per second) haversine waveform. During every loading session, each mouse was kept under isolfurane (2.5%, Ohmeda Cribe, Inc, Ohmeda Products Division Inc, NJ) anesthesia using IMPAC[6] (Integrated Multi Patient Anesthesia Center VetEquip, Inc. P.O. Box 10785, Pleasanton, CA). Due to differences in the mid-shaft tibial and ulnar cross-sectional size among breeds, the *in vivo* loads were customized to induce similar bending strain (deformation) within each loaded site.

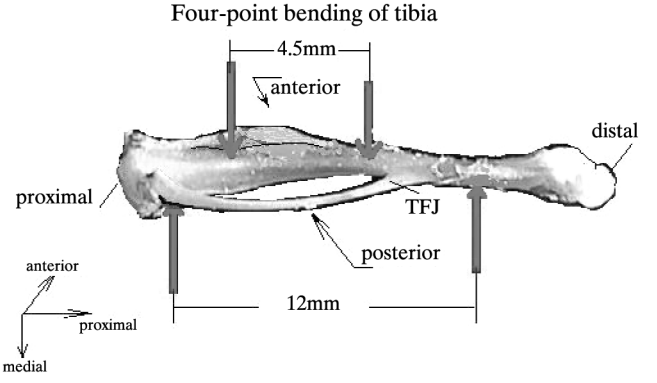

Figure 1. *In vivo* loading of tibia. Four-point bending of right tibia. Loading causes compressive strain/stresses on lateral surface and tensile strains/stresses on the medial surface.

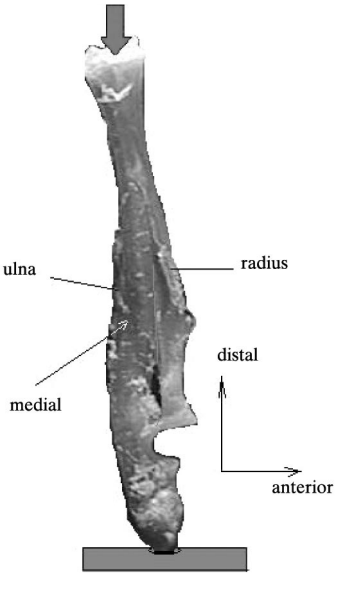

Figure 2. *In vivo* loading of right ulna. Loading causes compressive strain/stresses on medial surface and tensile strains/stresses on the lateral surface.

Tibia loading. The right leg of each of the animals was loaded externally such that the bending load was applied at the mid-tibial shaft using the four-point bending arrangement (Figure 1)[25,26,37,45]. Bending caused tensile strains on the medial surface and compressive strains on the lateral surface. The selected forces caused approximately 2000 microstrain (με) on the lateral surface of each tibia using 2.5 N in DBA and 3.5 N in B6 and C3 mice. The left legs of the mice served as non-loaded control. These mice were also subjected to *in vivo* ulnar loading on the same day.

(mean±SD)	Breed		
Bone site	B6	D2	C3
In vivo strain tibia (με/N)	587±90	780±130	570±115
In vivo strain slope ulna (με/N)	1127±159	1664±480	1020±171
με– microstrain; N – applied force in Newton.			

Table 1. Average mechanical strain on bone surface.

Ulnar loading. The right forearm (front limb) of each of the animals was loaded externally (Figure 2) such that the compression load was applied at the paw (distal ulnar joint) causing bending of the ulnar shaft[21]. Bending caused compression strains on the medial surface and tensile strains on the lateral surface. The selected forces were to induce approximately 2000 microstrain (με) at the mid-shaft ulna of each mouse breed. The selected forces were 1.5 N for DBA, and 2 N for C57BL/6J and C3H/HeJ mice ulnae (Figure 1). The left forearm of the mice was not loaded and served as non-loaded control.

To label or identify the new bone formation due to loading, the mice were given calcein injections on days 14 and 18 and were killed 21 days after the first loading.

C. Tissue collection

The right and left ulnae and tibiae were collected and placed in a 70% ethanol solution for subsequent processing and analyses by standard histomorphometry. A 3-mm segment was removed from each of the ends of tibiae and ulnae, and the remaining bone specimens were stained for three days in Villanueva stain and then dehydrated in graded ethanol and embedded in methyl methacrylate[25,26,37].

Physical measurements that included tibial and ulnar lengths, mid-shaft cortical area, marrow and second moment of area/inertia (around medial-lateral [ML] axis) were obtained within each breed. The raw data (average of left and right limb) from the physical measurements were compared among the three breeds.

The bone specimens were processed using standard protocols for histological undecalcified cortical bone slides[46]. Transverse sections of the ulnae and tibiae were taken using a saw microtome; the sections were 80 μm thick. Two sections of each tibia and ulna were given a blind code and randomized for analysis. To visualize the histomorphometric change, we used a light/epifluorescent microscope and digital camera. The data were measured using Bioquant 2000 Software. The data collected included marrow area, total area, periosteal and endocortical single and double calcein label, woven bone, width of double labels and total bone perimeter. The endpoints included calculated parameters of net bone formation due to loading. Net bone formation was calculated by subtracting the left (non-loaded) from the right (loaded) limb for each parameter. The normalized (net bone formation) standard histomorphometric variables include percentage mineralizing surface (%MS), mineral apposition rate (MAR), and bone formation rate (BFR).

D. Tibial and ulnar strain measurements

In a separate experiment, three mice per breed were subjected to direct mechanical strain measurements in the tibial (lateral) and ulnar (medial) periosteal surfaces using uniaxial strain gages (EA-09-032SG-120, Vishay, NC). Three gages per bone site, one at a time, were bonded to the bone surface using M-Bond-200 glue (Vishay, Raleigh, NC). Loads were applied to tibiae (1 to 4 N) (Figure 1) and ulnae (1 to 3 N) (Figure 2) to get average load-strain relationships (1/stiffness=με/N). The average load-strain relationship was then used to select *in vivo* bending loads for ulna and tibia loading.

E. Statistical analysis

Using two-way ANOVA with repeated measures, the differences were examined in all the endpoints 1) between the inbred mouse strains (B6, D2, C3), and 2) between sites (tibia and ulna). All differences were evaluated at a significance level of $p<0.05$, and marginal significance at $p<0.1$. All statistical analyses were performed using the statistical package SPSS for Windows v. 11 (SPSS Inc., Chicago, IL, USA).

Results

The average periosteal strain slope (1/stiffness) in ulnae of D2 (1664 με/N) was 48%, and 63% greater as compared to B6 and C3 respectively. The average periosteal strain slope (1/stiffness) in tibiae of D2 (780 με/N) was 33% and 37% greater as compared to B6 and C3 mice, respectively (Table 1). The calculations of strain slope (με/N) were based on the measured strain data and were then used to determine applied bending loads for limbs within each mouse breed.

The level of significant differences in the net (right limb – left limb) bone adaptation response variables (histomorphometry) were not reached among the 3 breeds (genotypes) either at the tibia or ulna (Table 2). The significant site-related differences were present within each mouse

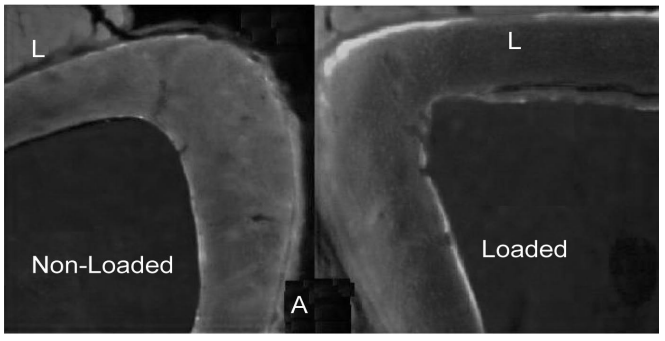

A. Tibial cross-sections 10X (B6)

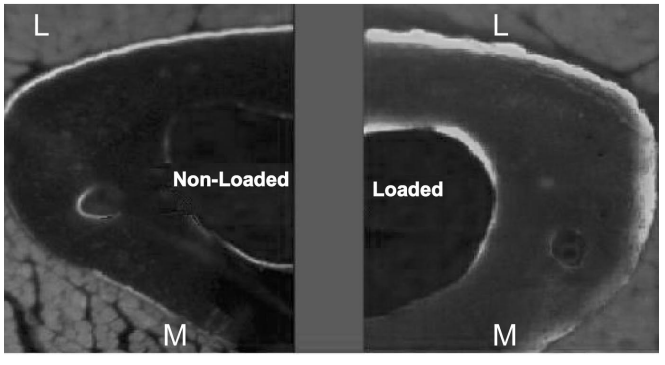

B. Tibial cross-sections 10X (D2)

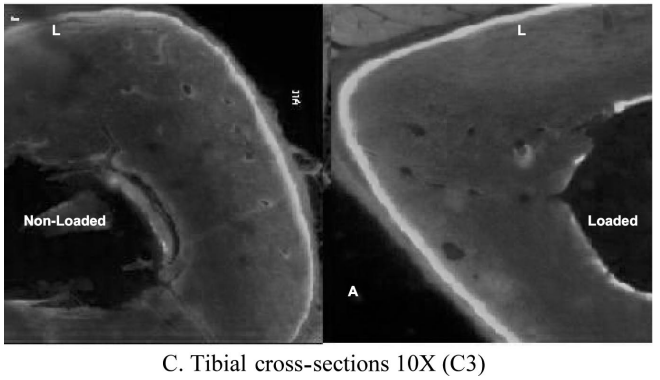

C. Tibial cross-sections 10X (C3)

Figure 3 (A-C). Transverse cross-section from mid-shaft tibia in three mouse breeds. Lateral (L) and medial (M) surfaces experienced compressive and tensile strains, respectively during the four-point bending (Figure 1) *in vivo*. The loaded right tibial cross-sections show relatively greater calcein label/bone formation as compared to non-loaded left tibia within each mouse breed (B6, D2, & C3).

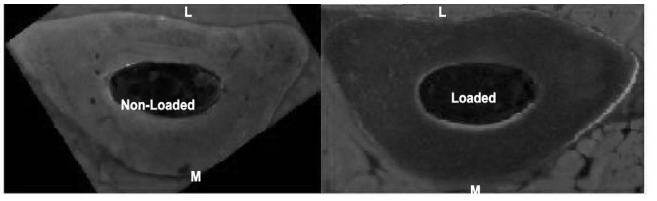

A. Ulnar cross-sections 10X (B6)

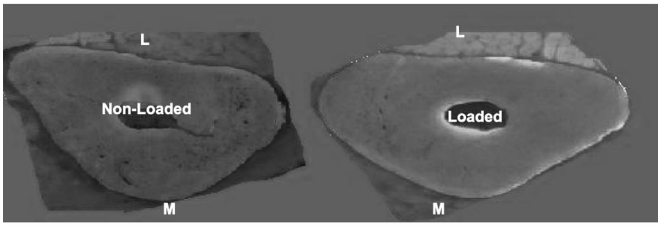

B. Ulnar cross-sections 10X (D2)

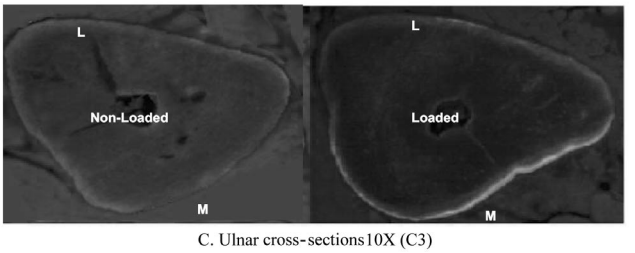

C. Ulnar cross-sections 10X (C3)

Figure 4 (A-C). Transverse cross-section from mid-shaft ulna in three mouse-breeds. Lateral (L) and medial (M) surfaces experienced tensile and compressive strains, respectively during the compression loading (Figure 2) *in vivo*. The loaded right ulnar cross-sections show relatively greater calcein label/bone formation as compared to non-loaded left ulna within each mouse breed (B6, D2, & C3).

breed ($p<0.05$). In all cases, the tibia showed greater %MS, MAR, and BFR than the ulna for similar mechanical strains (stresses) induced at the periosteal surfaces. There was no significant interaction between breed and site. For the same loading conditions (periosteal surface strain of ~2000 με), measures of %MS, MAR, and BFR were 1.6 to 27 fold greater at the tibia (Figure 3) than at the ulnar site (Figure 4) (Table 2).

Discussion

The site and breed-specific bone adaptation response was investigated in three mouse breeds using *in vivo* mechanical loading of tibia and ulna within each mouse breed. Similar bending strain magnitude in tibial and ulnar loading caused site-specific bone response differences within each mouse breed. Bone adaptation response to similar bending strain magnitude was greater in the tibia than in the ulna. It was expected that the bone adaptation response to mechanical stimulus (within each site) to be different among the three mouse breeds with the greatest in B6 and the least in the C3 mice[26,37,44,47-49]. However, there were no significant differences in bone adaptation response due to breed within each loaded site.

The site-specific bone adaptation response (bone formation) (Table 2, $p<0.05$) is also evident from bone labeling response, which is more distinct and greater in the tibial bone sections (Figure 3) as compared to the ulnar sections (Figure 4). Based on these data, it is suggested that additional studies should be done to evaluate tibial bending response to an *in vivo* loading that is similar to physiological

Breed	B6		D2		C3	
(mean±SD)	**Tibia**	***Ulna***	**Tibia**	***Ulna***	**Tibia**	***Ulna***
MS (%)	19.3±5.1[b]	7.2±2.4	15.3±2.9[b]	3.5±2.1	14.3±2.9[b]	6.8±3.1
MAR	0.85±0.4[b]	0.03±0.12	0.39±0.17[b]	0.15±0.15	0.20±0.05[b]	0.17±0.1
BFR	272±108[b]	30±12	187±53[b]	12±10	223±55[b]	37±19

[b] $p<0.05$ tibia vs. ulna; Results are adjusted mean±sem. **MS**=%; **MAR**=μm/d; **BFR**=$\mu m^3/\mu m^2$/yr

Table 2. Net bone response (right loaded–left non-leaded limb).

Breed (mean±SD)	**B6**	**D2**	**C3**
Body weights (g)	20.4±0.9	22.4±1.8[a]	22.8±1.4[a]
Tibia			
Length (mm)	18.4±0.97	18.5±0.84	19.1±1.02[a]
Total Area (mm^2)	1.0±0.16	0.68±0.05[a]	0.96±0.12[b]
Marrow Area (mm^2)	0.45±0.12	0.13±0.02[a]	0.16±0.05[a]
Cortical Area (mm^2)	0.59±0.14	0.55±0.04	0.80±0.09[ab]
Second moment of area (ML plane) 10^{-3} mm^4	66±9	39±6[a]	72±16[b]
Ulna			
Length (mm)	13.5±0.4	13.5±0.6	13.9±0.5[ab]
Total Area (mm^2)	0.3±0.04	0.24±0.06	0.24±0.033
Marrow Area (mm^2)	0.05±0.01	0.02±0.01[a]	0.008±0.002[ab]
Cortical Area (mm^2)	0.22±0.04	0.22±0.06	0.23±0.03
Second moment of area (ML plane) 10^{-3} mm^4	5.5±0.9	2.7±0.6[a]	3.6±0.4[a]
Second moment of area (maximum) 10^{-3} mm^4	22.0±6.5	11.7±4.8[a]	12.3±3.6[a]

[a] Different than B6, [b] Different than D2 ($p<0.05$). There were no differences between the left and right limb physical measurements. The raw physical data from left and right limbs were combined and averaged.

Table 3. Physical measurements.

weight/load bearing[42,51]. For example, similar to physiological load bearing, both ulnae and tibiae can be loaded and subjected to both compression and bending load[42,51].

Physiologically, hind limbs (tibiae) may be subjected to greater load-bearing from body weight than the forelimbs (ulnae). Therefore, it was expected that bone adaptation response might be different between the tibia and ulna when subjected to similar strain magnitude. It is possible that the tibial site is more responsive to loading and therefore provides relatively more robust adaptation response than the ulna. However, it is not known if the increased responsiveness to loading is either due to greater osteoblast cell density or greater cell sensitivity in tibia as compared to ulna. Either case will suggest that skeletal bone response is site-specific and should also be investigated in humans.

Although the induced bending strain magnitudes were similar in both the tibia and the ulna, the mode of creating bending load was different (Figure 1 and 2). While four-point bending causes local periosteal pressure[26,37] in tibial loading, we expect minimum bone response to pressure (or local periosteal compression) alone[23-25]. Therefore, bone response to similar bending strain in the tibia and the ulna are comparable. Unlike the ulna, the tibia continued to show greater responsiveness to loading. Furthermore, the tibia also showed increasing trends in the parameters of bone formation (%MS, MAR, BFR) in B6 as compared to both C3 and D2[26,37,44,47-49].

During physiological load-bearing, tibiae and ulnae get loading from compression, and undergo bending such that the periosteal surface have both bending and compression components along with some shear and torsion. Relatively tibiae are under greater compressive bending load (medial periosteal surface) than ulnae during normal load-bearing under body weight. Unlike tibiae, the ulnae were subjected to *in vivo* loading to produce strain distribution similar to the one expected from normal weight-bearing in mice. Despite non-physiologic loading during four-point bending[25,26,37], the tibiae showed greater responsiveness to loading then ulnae which were loaded more physiologically with compression and bending. Regardless of loading mode, both limb sites

subjected to similar bending strains/deformation, but resulted in different bone adaptation responses. It is also possible that even though similar strain/deformation was targeted, there may be breed-related differences in the load distribution (loading environment), and the induced strain may not have reached the target levels.

Although the induced strain is similar (~ 2000 με) at mid-shaft tibiae and ulnae within each mouse breed, its distribution may vary along the length. The breed-related differences in the strain distribution may also be due to a variation in size and shape of limbs among various mouse breeds. For instance, the ulnar and tibial lengths were greatest in C3 mice as compared to both B6 and D2 (Table 3). The mid-shaft tibial total area (marrow+cortical) was smallest in D2 as compared to both B6 and C3. Marrow area for both ulnar and tibial mid-shaft was greatest in B6 mice as compared to both D2 and C3. While cortical area was greatest in C3 tibiae, there was no difference at the ulnar site among all the breeds (Table 3). The second moment of area (in medial-lateral [ML] bending plane) was lowest in the DBA tibiae and greatest in the B6 ulnae (Table 3).

The true *in vivo* tibial and ulnar strain during normal ambulation under body weight is difficult to estimate without direct measurements (from strain gages). For instance, the B6 mice were lighter in body weight as compared to both D2 and C3 (Table 3) and yet the second moment of area (resistance to bending) was greatest in the ulna and it was greater than DBA in the tibia (Table 3). Therefore, it is essential to develop loading methods that will induce similar strain magnitude in the mid-shaft ulnae and tibiae in order to compare the site-specific adaptation responses.

The study of site-specific bone adaptation response to *in vivo* loading in the rat by Li et al.[40] compared the mid-shaft tibial endocortical to ulnar periosteal bone response. Although the periosteal surface stimulus was approximately 3000 microstrain, the ulnar and tibial periosteal response was not compared. In the current study, the direct comparison between the tibial and ulnar periosteal response allows us to understand the site-specific bone adaptation characteristics of the skeleton. Iwamoto et al.[50] showed that the exercise-related bone mass formation is greater in distal as compared to the proximal cancellous bone within each tibia suggesting a complex site-specific bone adaptation system which needs to be explored in future studies.

Robling's data suggested greater bone adaptation response of ulnae in B6 mice as compared to both C3 and D2 when subjected to compressive loading[21]. The current study did not find any significant breed-related differences in ulnar bone adaptation response, however, D2 showed declining trends in %MS and BFR as compared to B6 and C3. Unlike the data from tibia loading models[25,26], disuse[48], and ulna[21], the lack of significant differences in bone formation response among the three mouse breeds may be due to the complexity of the adaptation system responding simultaneously to mechanical stimulation at two different sites. This suggests that any systemic factors pertaining to one bone site may influence the loading response of another site. The bone adaptation response to exercise (mechanical stimuli) is a complex process that involves genotypes (breed), bone site, and other factors including age[33,43] and loading conditions where rest periods are added during loading[19,20,22].

In summary, these data provide an insight into the site-specific bone adaptation response of the skeleton in mouse animal models representing three breeds. Although limited data exist that may provide some clue to whether or not the human skeleton may have site-specific bone adaptation responses[29,41], we predict that the same could be true in humans as well. In conclusion, our data suggest that there are site-specific differences in bone adaptation response to similar mechanical stimulus.

Acknowledgements

We appreciate the help of Steve Short, Sara Morgan, and Daniel Wells, Adam Currier, and Andrew Manolides for their valuable help.

References

1. Slemenda CW, Christian JC, Williams CJ, Norton JA, Johnston CC Jr. Genetic determinants of bone mass in adult women: A re-evaluation of the twin model and the potential importance of gene interaction on heritability estimates. J Bone Miner Res 1991;6:561-7.
2. Pocock NA, Eisman JA, Hopper JL, Yeates MG, Sambrook PN, Eberl S. Genetic determinants of bone mass in adults. A twin study. J Clin Invest 1987;80:706-10.
3. Hoidrup S, Prescott E, Sorensen TI, Gottschau A, Lauritzen JB, Schroll M, Gronbaek M. Tobacco smoking and risk of hip fracture in men and women. Int J Epidemiol 2000;29:253-9.
4. Olofsson H, Byberg L, Mohsen R, Melhus H, Lithell H, Michaelsson K. Smoking and the risk of fracture in older men. J Bone Miner Res 2005;20:1208-15.
5. Qandil R, Sandhu HS, Matthews DC. Tobacco smoking and periodontal diseases. J Can Dent Assoc 1997; 63:187-92, 194-5.
6. Rundgren A, Mellstrom D. The effect of tobacco smoking on the bone mineral content of the ageing skeleton. Mech Ageing Dev 1984;28:273-7.
7. Aloia JF, Vaswani A, Yeh JK, Flaster E. Risk for osteoporosis in black women. Calcif Tissue Int 1996; 59:415-23.
8. Cosman F. Anabolic therapy for osteoporosis: Parathyroid hormone. Curr Osteoporos Rep 2005; 3:143-9.
9. Hodsman AB, Hanley DA, Ettinger MP, Bolognese MA, Fox J, Metcalfe AJ, Lindsay R. Efficacy and safety of human parathyroid hormone-(1-84) in increasing bone mineral density in postmenopausal osteoporosis. J Clin Endocrinol Metab 2003;88:5212-20.
10. Hodsman AB, Kisiel M, Adachi JD, Fraher LJ, Watson PH. Histomorphometric evidence for increased bone turnover without change in cortical thickness or porosi-

ty after 2 years of cyclical hPTH(1-34) therapy in women with severe osteoporosis. Bone 2000;27:311-8.
11. Lindsay R, Nieves J, Formica C, Henneman E, Woelfert L, Shen V, Dempster D, Cosman F. Randomised controlled study of effect of parathyroid hormone on vertebral-bone mass and fracture incidence among postmenopausal women on oestrogen with osteoporosis. Lancet 1997;350:550-5.
12. Ejersted C, Andreassen TT, Hauge EM, Melsen F, Oxlund H. Parathyroid hormone (1-34) increases vertebral bone mass, compressive strength, and quality in old rats. Bone 1995;17:507-11.
13. Lane NE, Kimmel DB, Nilsson MH, Cohen FE, Newton S, Nissenson RA, Strewler GJ. Bone-selective analogs of human PTH(1-34) increase bone formation in an ovariectomized rat model. J Bone Miner Res 1996;11:614-25.
14. Borer KT. Physical activity in the prevention and amelioration of osteoporosis in women: Interaction of mechanical, hormonal and dietary factors. Sports Med (Auckland, N.Z.) 2005;35:779-830.
15. Schroeder ET, Hawkins SA, Jaque SV. Musculoskeletal adaptations to 16 weeks of eccentric progressive resistance training in young women. J Strength Cond Res 2004;18:227-35.
16. Vico L, Alexandre C. Microgravity and bone adaptation at the tissue level. J Bone Miner Res 1992;7(Suppl.2): S445-7.
17. Turner CH, Robling AG. Exercise as an anabolic stimulus for bone. Curr Pharm Des 2004;10:2629-41.
18. Warden SJ, Hurst JA, Sanders MS, Turner CH, Burr DB, Li J. Bone adaptation to a mechanical loading program significantly increases skeletal fatigue resistance. J Bone Miner Res 2005;20:809-16.
19. Srinivasan S, Agans SC, King KA, Moy NY, Poliachik SL, Gross TS. Enabling bone formation in the aged skeleton via rest-inserted mechanical loading. Bone 2003;33:946-55.
20. Srinivasan S, Weimer DA, Agans SC, Bain SD, Gross TS. Low-magnitude mechanical loading becomes osteogenic when rest is inserted between each load cycle. J Bone Miner Res 2002;17:1613-20.
21. Robling AG, Turner CH. Mechanotransduction in bone: Genetic effects on mechanosensitivity in mice. Bone 2002;31:562-9.
22. Robling AG, Hinant FM, Burr DB, Turner CH. Improved bone structure and strength after long-term mechanical loading is greatest if loading is separated into short bouts. J Bone Miner Res 2002;17:1545-54.
23. Raab Cullen DM, Akhter MP, Kimmel DB, Recker RR. Periosteal bone formation stimulated by externally induced bending strains. J Bone Miner Res 1994; 9:1143-52.
24. Raab Cullen DM, Akhter MP, Kimmel DB, Recker RR. Bone response to alternate-day mechanical loading of the rat tibia. J Bone Miner Res 1994;9:203-11.
25. Akhter MP, Cullen DM, Recker RR. Bone adaptation response to sham and bending stimuli in mice. J Clin Densitom 2002;5:207-16.
26. Akhter MP, Cullen DM, Pedersen EA, Kimmel DB, Recker RR. Bone response to *in vivo* mechanical loading in two breeds of mice. Calcif Tissue Int 1998; 63:442-9.
27. Gross TS, Srinivasan S, Liu CC, Clemens TL, Bain SD. Noninvasive loading of the murine tibia: An *in vivo* model for the study of mechanotransduction. J Bone Miner Res 2000;17:493-501.
28. Torrance AG, Mosley JR, Suswillo RF, Lanyon LE. Noninvasive loading of the rat ulna *in vivo* induces a strain-related modeling response uncomplicated by trauma or periostal pressure. Calcif Tissue Int 1994; 54:241-7.
29. Hawkins SA, Schroeder ET, Wiswell RA, Jaque SV, Marcell TJ, Costa K. Eccentric muscle action increases site-specific osteogenic response. Med Sci Sports Exerc 1999;31:1287-92.
30. Judex S, Gross TS, Zernicke RF. Strain gradients correlate with sites of exercise-induced bone-forming surfaces in the adult skeleton. J Bone Miner Res 1997; 12:1737-45.
31. Cullen DM, Smith RT, Akhter MP. Bone-loading response varies with strain magnitude and cycle number. J Appl Physiol 1985 2001;91:1971-6.
32. Cullen DM, Smith RT, Akhter MP. Time course for bone formation with long-term external mechanical loading. J Appl Physiol 1985 2000;88:1943-8.
33. Forwood MR, Turner CH. Skeletal adaptations to mechanical usage: Results from tibial loading studies in rats. Bone 1995;17(Suppl.4):197S-205S.
34. Turner CH, Forwood MR, Rho JY, Yoshikawa T. Mechanical loading thresholds for lamellar and woven bone formation. J Bone Miner Res 1994;9:87-97.
35. Forwood MR, Turner CH. The response of rat tibiae to incremental bouts of mechanical loading: A quantum concept for bone formation. Bone 1994;15:603-9.
36. Rubin CT, Gross TS, McLeod KJ, Bain SD. Morphologic stages in lamellar bone formation stimulated by a potent mechanical stimulus. J Bone Miner Res 1995;10:488-95.
37. Pedersen EA, Akhter MP, Cullen DM, Kimmel DB, Recker RR. Bone response to *in vivo* mechanical loading in C3H/HeJ mice. Calcif Tissue Int 1999; 65:41-46.
38. Akhter MP, Raab DM, Turner CH, Kimmel DB, Recker RR. Characterization of *in vivo* strain in the rat tibia during external application of a four-point bending load. J Biomech 1992;25:1241-6.
39. Turner CH, Akhter MP, Raab DM, Kimmel DB, Recker RR. A noninvasive, *in vivo* model for studying strain adaptive bone modeling. Bone 1991;12:73-9.
40. Li J, Duncan RL, Burr DB, Gattone VH, Turner CH. Parathyroid hormone enhances mechanically induced bone formation, possibly involving L-type voltage-sensitive

calcium channels. Endocrinology 2003;144:1226-33.
41. Bennell KL, Malcolm SA, Khan KM, Thomas SA, Reid SJ, Brukner PD, Ebeling PR, Wark JD. Bone mass and bone turnover in power athletes, endurance athletes, and controls: A 12-month longitudinal study. Bone 1997;20:477-84.
42. Fritton JC, Myers ER, Wright TM, van der Meulen MC. Loading induces site-specific increases in mineral content assessed by microcomputed tomography of the mouse tibia. Bone 2005;36:1030-8.
43. Giangregorio L, Blimkie CJ. Skeletal adaptations to alterations in weight-bearing activity: A comparison of models of disuse osteoporosis. Sports Med (Auckland, N.Z.) 2002;32:459-76.
44. Sheng MH, Lau KH, Beamer WG, Baylink DJ, Wergedal JE. *In vivo* and *in vitro* evidence that the high osteoblastic activity in C3H/HeJ mice compared to C57BL/6J mice is intrinsic to bone cells. Bone 2004; 35:711-9.
45. Forwood MR, Bennett MB, Blowers AR, Nadorfi RL. Modification of the *in vivo* four-point loading model for studying mechanically induced bone adaptation. Bone 1998;23:307-10.
46. Parfitt AM. Bone histomorphometry: Standardization of nomenclature, symbols and units (summary of proposed system). Bone 1988;9:67-9.
47. Kodama Y, Umemura Y, Nagasawa S, Beamer WG, Donahue LR, Rosen CR, Baylink DJ, Farley JR. Exercise and mechanical loading increase periosteal bone formation and whole bone strength in C57BL/6J mice but not in C3H/Hej mice. Calcif Tissue Int 2000; 66:298-306.
48. Kodama Y, Dimai HP, Wergedal J, Sheng M, Malpe R, Kutilek S, Beamer W, Donahue LR, Rosen C, Baylink DJ, Farley J. Cortical tibial bone volume in two strains of mice: Effects of sciatic neurectomy and genetic regulation of bone response to mechanical loading. Bone 1999;25:183-90.
49. Beamer WG, Donahue LR, Rosen CJ, Baylink DJ. Genetic variability in adult bone density among inbred strains of mice. Bone 1996;18:397-403.
50. Iwamoto J, Yeh JK, Aloia JF. Differential effect of treadmill exercise on three cancellous bone sites in the young growing rat. Bone 1999;24:163-9.
51. De Souza RL, Matsuura M, Eckstein F, Rawlinson SC, Lanyon LE, Pitsillides AA. Non-invasive axial loading of mouse tibiae increases cortical bone formation and modifies trabecular organization: A new model to study cortical and cancellous compartments in a single loaded element. Bone 2005;37:810-8.